Identification of a Frenkel-pair defect in electron-irradiated 3*C* SiC

N. T. Son and E. Janzén
Department of Physics, Chemistry and Biology, Linköping University, SE-581 83 Linköping, Sweden

J. Isoya
Graduate School of Library, Information and Media Studies, University of Tsukuba, 1-2 Kasuga, Tsukuba, Ibaraki 305-8550, Japan

N. Morishita, H. Hanaya, H. Takizawa, and T. Ohshima
Japan Atomic Energy Agency, 1233 Watanuki, Takasaki, Gunma 370-1292, Japan

A. Gali
Budapest University of Technology and Economics, Budafoki út 8, H-1111 Budapest, Hungary
(Received 5 January 2009; revised manuscript received 31 July 2009; published 2 September 2009)

An electron paramagnetic resonance (EPR) spectrum labeled LE1 was observed in *n*-type 3*C* SiC after electron irradiation at low temperatures (~80–100 K). A hyperfine interaction with four nearest C neighbors similar to that of the well-known silicon vacancy in the negative charge state was observed, but the LE1 center has a lower symmetry, C_{2v}. Supercell calculations of different configurations of silicon vacancy-interstitial Frenkel-pairs, V_{Si}-Si_i, were performed showing that pairs with a nearest neighbor Si interstitial are unstable—V_{Si} and Si_i will automatically recombine—whereas pairs with a second neighbor Si_i are stable. Comparing the data obtained from EPR and supercell calculations, the LE1 center is assigned to the Frenkel-pair between V_{Si} and a second neighbor Si_i interstitial along the [100] direction in the 3+ charge state, V_{Si}^{-}-Si_i^{4+}. In addition, a path for the migration of Si_i^{4+} was found in 3*C* SiC. In samples irradiated at low temperatures, the LE1 Frenkel-pair was found to be the dominating defect whereas EPR signals of single vacancies were not detected. The center disappears after warming up the samples to room temperature.

DOI: 10.1103/PhysRevB.80.125201 PACS number(s): 61.72.jj, 61.72.jd, 71.15.Mb

I. INTRODUCTION

Radiation-induced defects in SiC have been extensively studied.[1,2] However, in most of the studies the irradiation was performed at room temperature or even higher temperatures and the self-interstitials (Si_i and C_i) may already be mobile at these temperatures. So far electron paramagnetic resonance (EPR) studies of defects induced by irradiation at low temperatures (77 K) were only reported for *p*-type 6*H* SiC by von Bardeleben and co-workers[3] and defects with spin S=3/2 and hyperfine (hf) interactions with nearest C neighbors were attributed to far-distance Si Frenkel-pairs (~6.5 Å between the silicon vacancy, V_{Si}, and a Si_i interstitial for the pair along the *c* axis).[3] The defects were observed only in samples irradiated with low-energy electrons (300 keV). Although the irradiation took place at 77 K, EPR measurements were performed at room temperature[3] so it is not clear if the defect was formed during irradiation at low temperatures or after the migration of interstitials. As shown from photoluminescence studies in samples irradiated at room temperatures, some intrinsic defects can be observed outside the irradiated region[4] indicating a possible migration of primary defects such as interstitials. Theoretical calculations predicted different configurations of isolated and split interstitials in 3*C* and 4*H* SiC.[5,6] Among different types of interstitial defects, isolated interstitials, and vacancy-interstitial Frenkel-pairs are expected to be less stable. In other semiconductors, Frenkel-paired defects are known to be annealed out at temperatures well below room temperatures. So far, the formation and stability of Frenkel-pairs in SiC have mainly been theoretically studied.[7–10] Simulations using molecular dynamics in 3*C* SiC (Refs. 7 and 8) suggest that Frenkel-pairs with the interstitial-vacancy distances less than the lattice constant a_0 (~4.36 Å) are not stable and that Si interstitials recombine more easily than C interstitials. The obtained activation energies for defect recombination processes were between 0.22 and 1.6 eV for C Frenkel-pairs and between 0.28 and 0.9 eV for Si Frenkel-pairs in those simulations.[8] The migration of interstitials in certain configurations and mostly in the *neutral* charge state have been studied by *ab initio* calculations in 3*C* SiC.[9,10] From theoretical studies it is expected that Frenkel-pairs with large interstitial-vacancy distances are stable and may be detected by experiments. Since beyond the nearest neighborhood, the hexagonal and cubic structures differ configurations of Frenkel-pairs and the migration paths for interstitials in 3*C* SiC may be different from those in 4*H* and 6*H* SiC. It is of interest to identify the stable configurations of Frenkel-pairs and to investigate the electronic structure of the vacancy perturbed by a nearby interstitial. In this study, we performed electron irradiation at low temperatures (~80–100 K) in order to create defects when interstitials may still be immobile and to minimize the formation of secondary defects and at the same time to enhance the chance of observing isolated interstitials or Frenkel-pairs. In order to reduce the complication in EPR study due to the presence of different defect configurations corresponding to different inequivalent lattice sites in the hexagonal polytypes (2 and 3 in 4*H* and 6*H* SiC, respectively), we used the simpler zinc-blende 3*C* SiC. In this paper we present our identification of a Frenkel-pair in 3*C* SiC based on the data obtained from EPR measurements and

supercell calculations. The formation of the defect and the migration paths for Si interstitials are discussed.

II. EXPERIMENTAL DETAILS

The samples used in our study are *n*-type 3*C* SiC layers grown by chemical vapor deposition on (100) Si substrates. Before the growth, countered slopes oriented in the [110] and $[\bar{1}\bar{1}0]$ directions were formed over the entire surface of the Si(100) substrate in order to eliminate planar defects in the 3*C* SiC layers. Details on the crystal growth can be found elsewhere.[11] Freestanding layers (~0.3 mm thick) were obtained by chemical etching of the Si substrates. The size of samples is $20\times3\times0.3$ in mm. The concentration of the N shallow donor is $\sim2\times10^{16}$ cm^{-3} as estimated by EPR. Irradiation with 2MeV electrons was performed at low temperatures to a dose of 5×10^{17} cm^{-3} with the electron beam parallel to the [100] direction. Our Monte Carlo simulations show that at the depth of 200 μm the electron beam spreads to ~250 μm in diameter (mostly concentrating in a region of ~130 μm in diameter). During irradiation, the samples were kept in a cryostat with continuous liquid-N_2 flow and the electron-beam-induced current was adjusted to keep the sample temperature in the range of 80–100 K. The samples were then transferred to specially designed sample tubes, which were evacuated and stored in liquid N_2. EPR measurements were performed using an E500 X-band Bruker spectrometer. All the spectra were detected under some sorts of light illumination since the cryostat was not optically sealed to facilitate sample transfer (sample is exposed to room light via the open top of the double-wall dewar in the cavity). The time for transferring the sample from the sample tube (kept at 77 K) to the cavity (kept at 15–20 K) for EPR measurements is typically ~3–4 seconds and the sample temperature is expected not to exceed 90–100 K during the transfer. White light illumination (halogen lamp) was used for optimizing the sample position in the cavity.

III. RESULTS AND DISCUSSION

Before irradiation, only the EPR spectrum of the N shallow donor was detected. After irradiation, the N spectrum disappeared and several EPR spectra were observed. Figures 1(a)–1(c) show the dominating spectra appearing in the magnetic-field region close to $g=2$ measured at 28 K under white light illumination for the magnetic field **B** along three main crystallographic directions. For **B**‖[100], the spectrum shows a strong central line with a typical hf structure due to the interaction with 12 next-nearest Si neighbors [Fig. 1(a)]. Two clear hf lines due to the interaction with four equivalent nearest C neighbors are also detected. The detailed structure can be seen in the insert (×10 scale) of the figure. Such hf structures are very similar to those of the Si vacancy in the negative charge state, V_{Si}^-.[10,11] Rotating the magnetic field away from the [100] direction, eight weaker EPR lines split off from the central line and join to four lines at **B**‖[111] and to five lines at **B**‖[011] [Figs. 1(b) and 1(c)]. These lines are labeled as LE1 and LE1′ (LE: low-temperature electron irradiation). The C hf lines are also split off and some of them

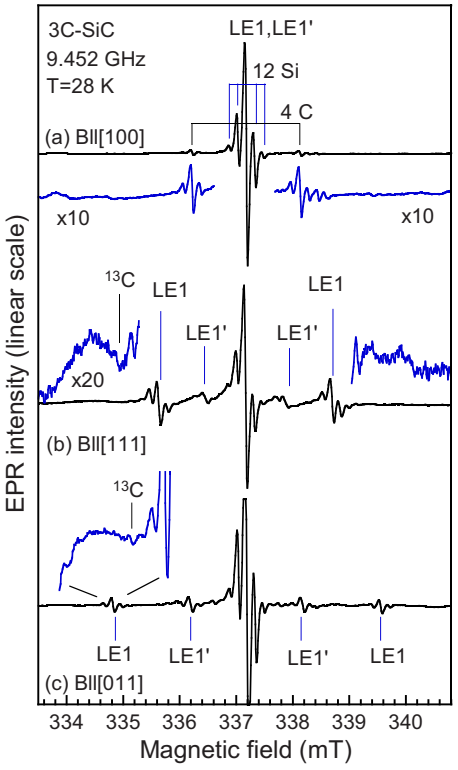

FIG. 1. (Color online) EPR spectra in 3*C* SiC after electron irradiation at ~80–100 K measured at 28 K under white light illumination for (a) **B**‖[100], (b) **B**‖[111], and (c) **B**‖[011]. The insets show the hf structures due to the interaction with the four nearest C neighbors. The insert in (c) is a scaled up part from the same spectrum showing also lower magnetic-field regions with a different scale.

can be followed for low- and high-field EPR lines. Neither the LE1 nor the LE1′ spectra were detected in samples irradiated at room temperature.

The LE1 and LE1′ spectra were not detected at temperatures above 60 K. Figures 2(a) and 2(b) show the spectra detected at 28 and 70 K, respectively, for **B**‖[100]. At 70 K, the LE1 and LE1′ disappeared and a signal labeled LE2 was detected [see the spectrum plotted with ×6 scale in Fig. 2(b)]. The LE2 has trigonal symmetry (C_{3v}) with an effective electron spin $S=1/2$ and g values: $g_{\|}=2.0023$ and $g_{\perp}=2.0035$. We will not discuss further on the LE2 center in this paper. Unexpectedly, no isotropic EPR signal that has the same g value and typical hf structure as the V_{Si}^- signal[12,13] could be detected at temperatures above 60 K when the LE1 and LE1′ disappear. Considering the well-known fact that in *n*-type 3*C* SiC irradiated at room temperature, the V_{Si}^- signal can be detected in the whole temperature range 4–300 K (see for example Ref. 13). Therefore, the missing of the V_{Si}^- signal at temperatures above 60 K in our samples indicates that the V_{Si}^- signal does not appear right after electron irradiation at low temperatures or its concentration is below the detection limit of our EPR system. We also noticed that in all our 15 samples of *n*- and *p*-type 4*H* and 6*H* SiC irradiated at low temperatures, no EPR signal of the single vacancies (V_{Si}^- or V_C^+)[14] could be detected in the studied temperature range 6–120 K (either in darkness or under light illumination).

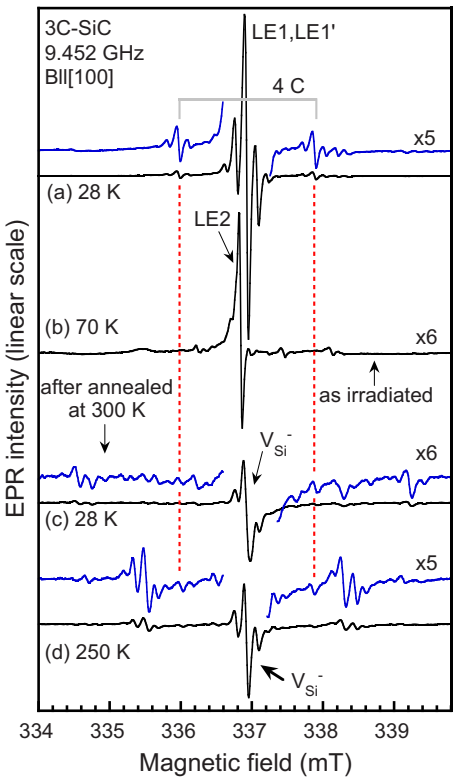

FIG. 2. (Color online) EPR spectra in 3*C* SiC measured for **B**∥[100] before (a–b) and after (c–d) warming up the sample to room temperature (~300 K). All the spectra were measured with the same parameters and microwave power.

After warming up the samples to room temperature (~300 K) both the LE1 and LE1′ spectra were annealed out [Figs. 2(c) and 2(d)]. This was confirmed from angular dependence studies which show only one isotropic line from V_{Si}^- at all angles of the magnetic field. As can be seen in Figs. 2(c) and 2(d), the main line becomes much weaker (about four times) and several EPR lines appear. At low temperatures, the main line is weak, slightly asymmetric, and broader due to overlapping of the V_{Si}^- and other unknown signals. The V_{Si}^- signal with its weak C hf structure can be detected in the whole temperature range 6–300 K, and becomes clearer when measuring at temperatures ~250 K [Fig. 2(d)]. Thus, the temperature-dependence study suggests that the central line observed before annealing is mainly from the LE1 defect (and possibly also LE1′) and no or negligible contribution from the V_{Si}^- signal. The LE1′ signal is weak and hence it is not clear whether the spectrum has also a line overlapping with the central line or not. Therefore, the spin state of the LE1′ center could not be unambiguously determined from the present experiment. In this paper, we limit our study on the identification of the LE1 defect and will not discuss further the LE1′ spectrum.

The angular dependences of the LE1 spectrum measured with **B** rotating in the $(0\bar{1}1)$ plane are plotted in Fig. 3 with the open circles representing experimental data points. This angular dependence is rather unusual with only one resonance at [100] and five ones at an arbitrary direction. As can be seen in Fig. 3, when rotating the magnetic field away from

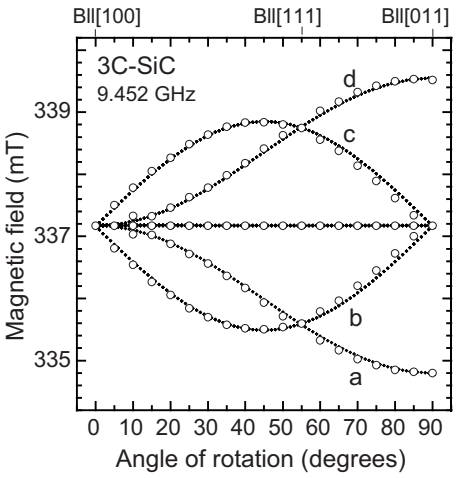

FIG. 3. Angular dependence of the LE1 spectrum in 3*C* SiC with the magnetic field rotating in the $(0\bar{1}1)$ plane. The dotted curves represent the simulated angular dependence using the parameters in Table I and the spin-Hamiltonian Eq. (7).

the [100] direction, the single line splits into four anisotropic lines (labeled a–d) and one isotropic central line. The measurements show that "a" and "d" are from two single defect orientations corresponding to two inequivalent g components which are not split by sample misalignment. The "b" or "c" line is contributed from two equivalent defect orientations and each splits into two lines in cases of a slight sample misalignment. (Such a sample misalignment often occurred and was corrected using a three-dimensional goniometry to eliminate the splitting of the lines b and c before recording the whole spectrum.)

In a cubic crystal, there are eight possible different symmetry systems[15] and the observed pattern of rotation at arbitrary directions for LE1 indicates C_{2v} symmetry. No other symmetries can have an angular dependence with one single loop and one double loop.[15] However, this is a special case of C_{2v} symmetry, which can be understood by considering the case of $S=1/2$ (the central line is not included). Choosing the principal axis system in which the g tensor is diagonal, the angular dependence described in g values has the form

$$g = [(g_1 \cdot l)^2 + (g_2 \cdot m)^2 + (g_3 \cdot n)^2]^{1/2} \quad (1)$$

here l, m, and n are the direction cosines of the magnetic field with respect to the principle axes of the g tensor (the principal axes of g_1, g_2, and g_3 are along the [100], [011], and $[0\bar{1}1]$ or equivalent directions). In a cubic crystal, a C_{2v} center has six defect orientations and their g values can be described via three principal values g_1, g_2, and g_3. With **B** rotating in the $(0\bar{1}1)$ plane, two of them are equivalent and the number of independent g components reduces to four. The g values for these four inequivalent orientations, $g_{a\text{-}d}$, can be written as

$$g_a = \{[g_1 \cos(\theta)]^2 + [g_2 \sin(\theta)]^2\}^{1/2} \quad (2)$$

$$g_d = \{[g_1 \cos(\theta)]^2 + [g_3 \sin(\theta)]^2\}^{1/2} \quad (3)$$

$$g_b = \{[g_1 \cos(45°)\sin(\theta)]^2 + [g_2 \cos(30°)\cos(\theta - \alpha)]^2 + [g_3 \cos(30°)\cos(\theta + \alpha)]^2\}^{1/2} \quad (4)$$

$$g_c = \{[g_1 \cos(45°)\sin(\theta)]^2 + [g_2 \cos(30°)\cos(\theta + \alpha)]^2 + [g_3 \cos(30°)\cos(\theta - \alpha)]^2\}^{1/2}. \quad (5)$$

Here θ is the angle between the magnetic field and the [100] direction, α is the angle between the [100] and [211] directions (the angles are in degrees and $\alpha = 35.264389627°$), and b and c are the two double orientations. For $\mathbf{B} \| [100]$, replacing $\theta = 0°$ in Eqs. (2)–(5) we have $g_a = g_d = g_1$ and $g_b = g_c = [(g_2^2 + g_3^2)/2]^{1/2}$. Normally, it will give rise to two separate resonance lines at [100] corresponding to g_1 and $[(g_2^2 + g_3^2)/2]^{1/2}$. However, if

$$g_1^2 = (g_2^2 + g_3^2)/2 \quad (6)$$

these two resonance lines will coincide. For $\mathbf{B} \| [011]$ ($\theta = 90°$), $g_a = g_2$, $g_d = g_3$, and $g_b = g_c = [(g_1^2/2) + (g_2^2 + g_3^2)/4)]^{1/2} = g_1$ [under the condition in Eq. (6)]. There will be three resonance lines; one appears exactly in the same position as for the [100] direction ($g_{b,c[011]} = g_{b,c[100]} = g_1$) and the other two appear at lower and higher magnetic fields with g values equal to g_2 and g_3, respectively. This type of angular dependences is observed in our experiments for the LE1 center. As also described in detail in Ref. 15, $g_{a,d}$ and $g_{b,c}$ (or labeled as S_1 and S_2, respectively, in Ref. 15) coincide at [100] only in the cases of C_{3v} and T_d symmetry (looking from the [100] direction the distortions along any of the ⟨011⟩, ⟨100⟩ and ⟨111⟩ or equivalent directions is symmetric). When the symmetry of an isolated defect lowers from T_d to C_{2v}, e.g, due to the Jahn-Teler effect, the distortion can occur randomly along any of the ⟨100⟩ or equivalent directions. Looking at one of the ⟨100⟩ directions, these distortions are seen differently and there will be two separated resonances observed for $\mathbf{B} \| \langle 100 \rangle$ (S_1 and S_2 in Ref. 13). The coincidence of these two resonances at [100] as observed for the LE1 center indicates that the distortion occurs preferentially only along [100]. We underline that the [100] axis is the direction of the applied electron irradiation that created the LE1 center.

As shown above, the central line also belongs to the LE1 spectrum, so the spin of the center should be $S = 3/2$. Its angular dependence can be described by the spin-Hamiltonian

$$H = \mu_B \mathbf{B} \cdot \mathbf{g} \cdot \mathbf{S} + D[S_{zz}^2 - S(S+1)/3] + E(S_{xx}^2 - S_{yy}^2) \quad (7)$$

here D and E are the fine-structure parameters representing the zero-field splitting caused by the axial and orthorhombic crystal fields, respectively, with $D = 3D_{zz}/2$ and $E = (D_{xx} - D_{yy})/2$. The fit to the experimental data of the LE1 center gives an isotropic g value $g = 2.0029$ and the fine-structure parameters $D = 11.1 \times 10^{-4}$ cm^{-1} and $E = -3.7 \times 10^{-4}$ cm^{-1}. With the typical line width of ~0.05–0.06 mT and the maximum error of ≤0.01 mT in the fits, the error in the g value is about ±0.0001. The error in the determination of D and E is about $\pm 0.09 \times 10^{-4}$ cm^{-1}. The spin-Hamiltonian parameters of LE1 are summarized in Table I. The D and E parameters were found to have opposite signs, i.e., either positive D and negative E or vice versa, but their absolute signs could not be determined from our experiments. The simulated angular dependence of the LE1 center using the parameters in Table I and the spin-Hamiltonian Eq. (7) is plotted in Fig. 3 as dotted curves.

TABLE I. Spin-Hamiltonian parameters for the LE1 defect in 3*C* SiC. The fine-structure parameters D, E, and the principal values of the hf tensor "*A*" are measured in the unit of 10^{-4} cm^{-1}. The principal z axis of the A tensor is parallel to the [111] direction. The parameters of V_{Si}^- [13] are also given for comparison. The calculated principal hf values for the $(V_{Si}\text{-}Si_i)^{3+}$ Frenkel-pair are given in parentheses. $\eta^2\alpha^2$ and $\eta^2\gamma^2$ are the spin densities in the $2s$ and $2p$ orbital, respectively, on a nearest C neighbor. The parameters D and E have opposite signs (positive D and negative E or vice versa) which could not be determined from the fits. The principal axis of the D tensor is along the [011] or equivalent directions. The error is ±0.0001 for the g values, ±0.09 10^{-4} cm^{-1} for D and E, and ±0.9 10^{-4} cm^{-1} for the A values.

	V_{Si}^-	LE1
Symmetry	T_d	C_{2v}
Spin	3/2	3/2
g	2.0029	2.0029
D		11.1
E		−3.7
A_{xx}	11.0	10.9 (13.9)
A_{yy}	11.0	10.9 (14.1)
A_{zz}	26.7	26.8 (29.6)
$\eta^2\alpha^2$ (%)	1.29	1.29
$\eta^2\gamma^2$ (%)	14.6	14.8
$\Sigma\,\eta^2(\alpha^2+\gamma^2)$	63.6	64.3

The hf interaction with the four nearest C neighbors can be followed for the outer lines of the LE1 center. At the angles between 0–50° from the c axis, the LE1 signal is rather strong and the C hf lines can be followed at most angles. The signal gets weaker at angles close to the [011] direction and the C hf lines are more difficult to follow as seen from the inserts in Figs. 1(b) and 1(c) (scaling up from a single long scan with a low modulation amplitude of 0.04 mT). The angular dependence of the hf splittings are plotted in Fig. 4. The least-square fit of the data gives the principal values of the hf tensor: $A_{zz} = A_\parallel = 26.8 \times 10^{-4}$ cm^{-1} = 80.4 MHz and $A_{xx} = A_{yy} = A_\perp = 10.9 \times 10^{-4}$ cm^{-1} = 32.8 MHz. Within the experimental error ($\pm 0.9 \times 10^{-4}$ cm^{-1}), the principal A values of the LE1 center are coincident with those of the V_{Si}^- center[12,13] ($A_\parallel = 26.7 \times 10^{-4}$ cm^{-1}, $A_\perp = 11.0 \times 10^{-4}$ cm^{-1}). The data for the V_{Si}^- center are also given in Table I for comparison.

Following the one-electron linear-combination-of-atomic-orbitals (LCAO) approximation, the wave function of the unpaired electron close to a neighboring C atom can be written as a superposition of the electronic wave function (ψ_s, ψ_p) of the s and p orbitals of the C atom

$$\Psi = \eta(\alpha\psi_s + \gamma\psi_p). \quad (8)$$

This wave function gives rise to a hyperfine interaction with isotropic and anisotropic components, which can be related

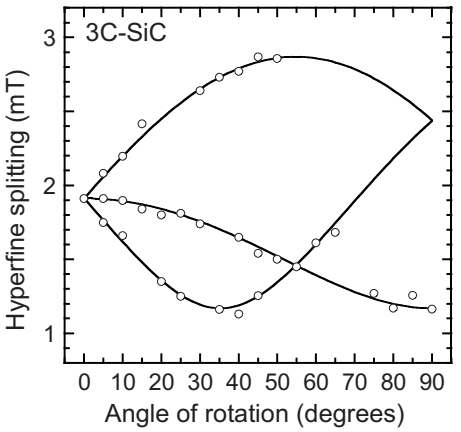

FIG. 4. The angular dependence of the ^{13}C hf splittings of the LE1 center measured with **B** rotating in the $(0\bar{1}1)$ plane.

to the unpaired spin in the *s* and *p* orbitals, respectively. The decomposition of the hyperfine tensor into isotropic and anisotropic parts can be written as

$$A = a\mathbf{1} + \boldsymbol{b}. \tag{9}$$

The trace *a* of the *A* tensor, the Fermi contact term, is determined by the spin density $\eta^2\alpha^2$ in the *s* orbital by the expression

$$a = (1/3)(A_{\parallel} + 2A_{\perp}) = (2/3)\mu_0 g \mu_B g_N \mu_N \eta^2 \alpha^2 |\psi_s(0)|^2. \tag{10}$$

The traceless anisotropic part $\boldsymbol{b}$ is an axial tensor with principal values $(2b,-b,-b)$, where

$$b = (1/3)(A_{\parallel} - A_{\perp}) = (1/4\pi)\mu_0 g \mu_B g_N \mu_N \eta^2 \gamma^2 (\pm 2/5)\langle r^{-3}\rangle_p. \tag{11}$$

Here μ_N is the nuclear magneton and g_N the nuclear *g* value of the ^{13}C isotope. From the principal *A* values, *a* and *b* were deduced as $a=48.7$ MHz and $b=15.9$ MHz. Using atomic constants given by Morton and Preston,[16] g_N value as tabulated by Fuller[17] and hf parameters from Table I, the spin densities $\eta^2\alpha^2$ and $\eta^2\gamma^2$ in the $2s$ and $2p$ orbitals on a nearest C neighbor are found to be 0.0129 (1.29%) and 0.148 (14.8%), respectively. This gives the total spin density on the four nearest C neighbors to be 0.643 or 64.3%, which is about the same for the case of V_{Si}^- (~63.6% as deduced from the principal hf values given in Ref. 13).

From the *g* values, the hf interaction, the effective electron spin $S=3/2$ as well as the localization of the spin density on the four nearest C neighbors it can be concluded that LE1 is very similar to V_{Si}^-. It is likely that LE1 is the V_{Si}^- $(S=3/2)$ being perturbed by a defect situated preferentially along the [100] direction that lowers the symmetry from T_d to C_{2v}, i.e., a pair involving V_{Si}^- and a defect with T_d symmetry lying along the [100] direction. Since the spin localizations of LE1 and V_{Si}^- are the same (within the experimental error), the spin density on the other component of the pair must be negligible. Therefore, the second component may not be a vacancy but is likely a nonbonded atom, most probably a Si interstitial ion with all four electrons being ionized.

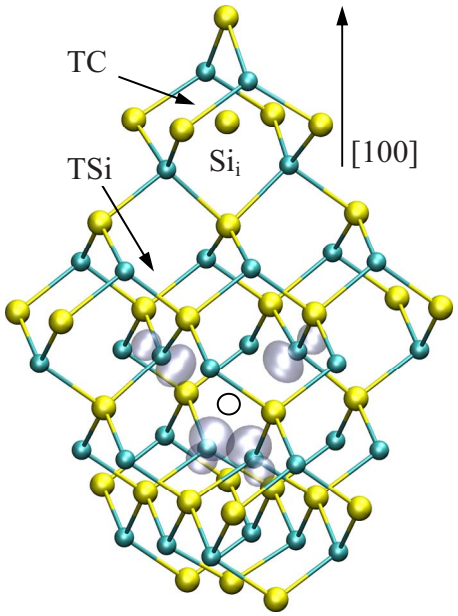

FIG. 5. (Color online) The defect model for the LE1 center: the Si vacancy-interstitial Frenkel-pair with the second neighbor Si_i at TC site along the [100] direction. The open circle denotes the vacant site. The selected isosurface of the calculated spin density is also shown: it is mainly localized on the four nearest C neighbors of the vacancy.

The most probable model for the LE1 center is the [100] Si Frenkel-pair in the 3+ charge state with a completely ionized Si_i (Si_i^{4+}) and a V_{Si}^- (trapping one electron), V_{Si}^--Si_i^{4+}. In this model, $S=3/2$ and the spin density is localized around the vacancy. This Frenkel-pair defect became our working model that reflects the conditions of the creation of the LE1 center.

Next, we investigate the stability and spin density of Si Frenkel-pairs in 3*C* SiC by *ab initio* calculations. We performed calculations using a 216 atom supercell with $2\times2\times2$ Monkhorst-Pack[18] *K*-point sampling. We applied local-density approximation within density-functional theory (DFT-LDA).[19,20] The geometry was optimized by VASP code[21] while the hyperfine tensors were determined by CP-PAW code[22] using projector augmented wave methodology[23] and plane-wave cutoff of 30 Ry. This method was proven to be very successful in identification of defects in 4*H* SiC.[24–26]

According to the measurements the LE1 defect has C_{2v} symmetry. Therefore we seek for the Frenkel-pair in this configuration. In order to fulfill this criterion, the silicon interstitial should be placed along the ⟨100⟩ or equivalent directions where the vacant site and the Si interstitial are along the common rotation axis. If the isolated Si interstitial was along the ⟨100⟩ direction then the Si interstitial has a stable configuration at the tetrahedral *T* site of the cubic lattice.[5] In the 3*C* SiC lattice there are two different *T* sites, caged by four C atoms (TC) or by four Si atoms (TSi). The TC site has a common rotation axis with the Si vacant site along ⟨100⟩ direction, while the TSi site is off axis (see Fig. 5). Therefore, the V_{Si}-Si_i(TC) Frenkel-pair is a suitable candidate for the LE1 EPR defect. The isolated Si interstitial will be 4+ charged at the TC site.[5] This shows that the Si interstitial can be easily positively ionized at the TC sites. On the other

hand, the isolated V_{Si} center can be negatively charged.[5,27,28] In the neutral charge state of V_{Si}, a t_2 level appears in the band gap close to the valence-band edge and is occupied by two electrons. Theoretically, one can put four additional electrons to this defect level. Roughly speaking, the neutral Si Frenkel-pair consisting of a V_{Si} and a Si interstitial at a TC site can be described as a $(V_{Si}^{4-}\text{-}Si_i^{4+})$ pair, where the low t_2 defect level of V_{Si} takes all the valence electrons of the Si interstitial atom. According to the prediction of the theory, the isolated V_{Si} can only be in the negative charge state in moderate *p*-type and *n*-type cubic SiC and is in the 2− charge state in *n*-type cubic SiC.[5,27] Following our simple arguments, this indicates that the neutral $(V_{Si}^{4-}\text{-}Si_i^{4+})$ *pair will not be stable*, but $(V_{Si}^{2-}\text{-}Si_i^{4+})=(V_{Si}\text{-}Si_i)^{2+}$ and $(V_{Si}^{-}\text{-}Si_i^{4+})=(V_{Si}\text{-}Si_i)^{3+}$ will be stable. The latter charge-state mimics the isolated V_{Si}^{-} defect which has the unique $S=3/2$ spin state in SiC. Thus, this defect with 3+ charge state became our working model for the LE1 EPR center. First, we placed the interstitial Si to the nearest-neighbor TC site of the silicon vacancy. We note here that the distances between a Si vacant site and the corresponding TC sites along the common [100] axis are the following: $0.5a_0$, $1.5a_0$, and $2.5a_0$. Thus, the nearest TC site is only about 2.2 Å away from the Si vacant site. We found that this configuration is unstable and Si_i will automatically recombine with the vacancy. This was previously found in neutral charge state, too.[7–10] Next, we put the interstitial Si to the next-nearest-neighbor TC site (see Fig. 5). This configuration is stable. We calculated the barrier energy for recombination. We used the drag method for barrier calculation where the reaction coordinate was along the [100] axis. The calculated barrier energy is about 2.4 eV for $(V_{Si}\text{-}Si_i)^{3+}$. We note that Si Frenkel-pairs have earlier been investigated in cubic SiC by using classical molecular dynamics[7,8] and by first-principles calculations.[9,10] However, these studies considered either other configurations[7,9] or this configuration but only in its neutral charge state.[10] Especially, Lucas and Pizzagalli found a very similar path to ours for the recombination of the neutral $V_{Si}\text{-}Si_i$(TC) pair by *ab initio* calculations.[10] Our combined EPR and theory studies indicate that the Si Frenkel-pair exhibit (3+) charge state, therefore, we believe that our calculated value, 2.4 eV, is the relevant energy needed for direct recombination.

After establishing the stable Si Frenkel-pair we analyze its electronic structure. This Si Frenkel-pair has C_{2v} symmetry. However, the perturbation on V_{Si} due to the interstitial Si is very small. Theoretically, there are two pairs of nearest-neighbor C atoms around the vacant site in C_{2v} symmetry, but the local symmetry remained T_d almost perfectly within 0.001 Å. The t_2 level will split, in this case marginally (within 0.07 eV), into a_1, b_1, and b_2 levels when lowering the symmetry from T_d to C_{2v}. By putting one electron in each of these levels, all with parallel spins, the high-spin multiplet state $^4A_2$ will be formed, which is very similar to the isolated V_{Si}^{-} as was argued above. The calculated hf constants of the nearest neighbor C atoms are: $A_{xx}=13.9\times10^{-4}$ cm^{-1} $=41.7$ MHz, $A_{yy}=14.1\times10^{-4}$ cm$^{-1}=42.3$ MHz, and $A_{zz}=29.6\times10^{-4}$ cm$^{-1}=88.8$ MHz. The calculated hf constants agree with the measured principal hf values of the LE1 EPR center ($A_{\perp}=10.9\times10^{-4}$ cm^{-1} and $A_{\parallel}=26.8\times10^{-4}$ cm^{-1}). The slightly larger calculated values are expected due to a limited size of the supercell (216 atoms). The hf constants of the interstitial Si were found to be negligible in the calculations as expected from the electronic structure of the defect. (Si_i is completely ionized and does not form covalent bonds to any neighboring atoms.)[5] Based on the agreement between EPR data and calculations, we identified the LE1 center as the Si Frenkel-pair with the second-neighbor Si_i in one of the [100] direction in the 3+ charge state, $(V_{Si}\text{-}Si_i)^{3+}$. We also calculated the $(V_{Si}\text{-}Si_i)^{4+}$ and $(V_{Si}\text{-}Si_i)^{2+}$ defects in this configuration. Both have $S=1$ ground state such as for V_{Si}^{0} and V_{Si}^{2-}. The calculated DFT-LDA occupation levels are at ~0.53 eV and ~1.25 eV above the valence-band maximum (VBM) for $(4+|3+)$ and $(3+|2+)$, respectively. These values are without any charge correction or DFT-LDA gap error correction. While the DFT-LDA gap error and charge corrections can partially compensate each other, it is expected that these occupation levels shift down closer to VBM because of the high charge states.[5]

Comparing the results obtained in our studies of 3*C* SiC and in studies of 6*H* SiC by von Bardeleben and co-workers,[3] one can see the following differences. We observed the [100] Si Frenkel-pairs in 3*C* SiC irradiated with high-energy electrons (2 MeV) along the [100] direction, whereas in Ref. 3, Frenkel-pairs with principal axes along the *c* direction or ~24° off can only be observed in samples irradiated with low-energy electrons along the *c* direction. With irradiation along the *c* direction by high-energy electrons, the Si (or C) atom being kicked out by electrons will have enough energies to kick out the next C (or Si) atom along the line to form a vacancy-antisite pair $V_{Si}\text{-}Si_C$ (or $V_C\text{-}C_{Si}$) and a C (or Si) interstitial. Therefore, Frenkel-pairs are not formed. In samples irradiated with low-energy electrons, the kicked-out Si (or C) atom has not enough energy to replace the next C (or Si) atom and therefore remains at interstitial positions. The close interstitials will recombine with the vacancy at room temperature and only the ones at far distances (~4.5 Å for inclined pairs and ~6.5 Å for axial pairs) will form the observed Frenkel-pairs.[3] In our study of 3*C* SiC, high-energy electrons kick out a Si atom and give it energy to continue their way along the [100] direction. This Si atom will then kick the next Si along the line (at $a_0=4.36$ Å away from the vacancy) and replace the position. As the result, the process leads to the formation of a Frenkel-pair between a Si vacancy and a next-nearest Si interstitial along the [100] direction (at a distance of $1.5a_0=6.54$ Å from the vacancy). If the low-energy irradiation is along the ⟨111⟩ or equivalent directions in 3*C* SiC then Frenkel-pairs similar to what observed in 6*H* SiC (Ref. 1) are expected to form.

As shown above from the observed data for the LE1 center, the spin density is mainly at V_{Si}. In the case of 1- charge state of V_{Si}, a fully occupied a_1 defect level appears in the valence band while the quasidegenerate t_2 state in the gap is occupied by three electrons. This defect state is strongly localized on the four C dangling bonds of the Si vacancy. No unpaired electron is localized at the Si interstitial of the Si Frenkel-pair. Therefore, the dipole-dipole interaction along the principal axis of the defect ([100]) connecting two components is negligible. The fine-structure parameters D and E are determined by the dipole-dipole and exchanged interac-

tion between spins of three unpaired electrons at four C dangling bonds. Every combination of two C dangling bonds makes a pair in a (011) or equivalent planes. The interaction between the spins at different dangling bonds is therefore more pronounced in the ⟨011⟩ or equivalent directions which determine the principal axis of the D tensor. The relative large E compared to D parameter in the case of LE1 center could be due to fact that the defects were created preferentially with C_{2v} distortion along [100] which is the direction of the electron beam. The random distribution of the defect in the [010] and [001] orientations may be negligible. This may somehow creates a stronger orthorhombic field preferentially in the [100] direction of the crystal lattice which results in relative large E parameters representing the zero-field splitting due to the orthorhombic field. The fine-structure parameters of the Frenkel-pairs are indeed the parameters of the single negative perturbed Si vacancy. Due to the high-symmetry T_d the unperturbed vacancy has no zero-field splitting. The perturbation of the Si interstitial in the Frenkel-pair lowers the symmetry of the defect to C_{2v} and hence induces the zero-field splitting of the single vacancy. The amplitude of the fine-structure parameters of LE1 center ($D=11.1\times10^{-4}$ cm^{-1}) is in the same range of D parameters of the V_{Si}^- centers in 4*H* SiC (35.1 MHz or 11.7×10^{-4} cm^{-1} for T_{V2a} center[29] and 0.009 μeV or 0.73×10^{-4} cm^{-1} for the T_{V1a} center).[30]

The calculated energy barrier for the Si interstitial at the second-nearest TC site to recombine with the vacancy is ~2.4 eV. Basically, the recombination process involves a kick-out mechanism in which the Si_i^{4+} at the TC site kicks out a Si atom from the lattice along the [100] direction toward the vacancy, that in turn becomes Si_i^{4+} at the nearest TC site and the original interstitial Si substitutes its place. This migration path for Si_i^{4+} has not yet been considered before in 3*C* SiC and has about 1.0 eV lower barrier energy than that of the other mechanisms.[5] Thus, this combined EPR and theoretical study revealed a path for the migration of isolated Si_i^{4+}. The Frenkel-pair can also be easily created by this kick-out mechanism: the barrier energy of 2.4 eV can be gained during our irradiation, especially, the applied electron beam was parallel to the [100] direction of the crystal. With the energy of 2 MeV, electrons can kick out a Si atom from its site (creating a vacancy) which in turn kicks out the next Si atom along the [100] axis to the interstitial position and replaces its site, finally forming a [100] Si TC interstitial defect near a Si vacancy. Thus, the formation of this Frenkel-pair defect is well understood. Apparently, the low stability of this Frenkel-pair defect cannot be explained by direct recombination possessing too high-energy barrier. First-principles calculations on the isolated Si vacancy showed similar or even higher barrier energy for diffusion,[9] therefore, the constituents of this Frenkel-pair defect would not move away and dissociate at room temperature. We speculate on two possible processes that can be responsible for the disappearance of this Frenkel-pair defect. (i) By raising the temperature the carbon interstitials with very low barrier energy[9] start to move and recombine with the carbon vacancy and the silicon vacancy as well with removing the Frenkel-pairs, too. In the latter case a carbon antisite is created which is electrically inactive. The diffusing carbon interstitials can also form thermally stable complexes with the silicon interstitials.[31] (ii) Due to the process (i) most of the defects are annihilated even at very low temperatures and the quasi Fermi-level increases with approaching the nominal doping level in our *n*-type sample. Then, the Si_i^{4+} defect will be unstable[9] and during autoionization it can diffuse away from the Si vacancy. Unfortunately, these processes are very complicated and beyond our computational capacity or methodology using *ab initio* calculations. Nevertheless, we believe that both scenarios are quite feasible and in line with the experience of previous studies.

IV. SUMMARY

In summary, we have observed a C_{2v}-symmetry EPR defect, LE1, in *n*-type 3*C* SiC irradiated with electrons in the [100] direction at ~80–100 K. The LE1 center has the same *g* values and similar hf interactions with four nearest C neighbors as the V_{Si}^- center. Supercell calculations of different configurations of the Si Frenkel-pair show that only the pair with a second-neighbor Si interstitial is stable in 3*C* SiC. Comparing the electronic structure and the hf constants obtained from EPR and supercell calculations, the LE1 center was identified as the Si Frenkel-pair with a second-neighbor Si interstitial at TC site along the [100] directions in the 3+ charge state, $(V_{Si}\text{-}Si_i)^{3+}$. In the 3+ charge state, the Si interstitial is completely ionized and the vacancy traps one electron. Without bonding to any neighboring atoms, the Si interstitial has a negligible perturbation on the localization of the spin density around the vacancy. Thus, Si_i interstitials at tetrahedral sites are indirectly detected through the identification of the perturbed vacancies in Frenkel-pairs. The perturbation of the Si interstitial lowers the symmetry of the system and leads to the detection of the fine-structure parameter D which represents the spin-spin interaction of V_{Si}^- that is not observable for the unperturbed V_{Si}^- center due to high T_d symmetry. This also explains why the principal axis of the D tensor is along ⟨011⟩ or equivalent directions [pairs of dangling bonds where electron spin density is localized in the (011) or equivalent planes] and does not coincide with the vacancy-interstitial axis along the [100] direction. Our results also show that in samples irradiated at low-temperatures Frenkel-pairs are dominating defects whereas EPR signals of single vacancies are absent.

ACKNOWLEDGMENTS

Support from the Swedish Foundation for Strategic Research, the Swedish Research Council, the Swedish National Infrastructure for Computing (Grant No. SNIC 011/04-8), and the *Gaikokujin kenkyuin* program at University of Tsukuba is acknowledged. A.G. acknowledges the Hungarian grant OTKA No. K-67886 and the Bolyai program of the Hungarian Academy of Sciences. The authors thank Hoya Corporation for 3*C* SiC samples.

[1] J. Isoya, T. Umeda, N. Mizuochi, N. T. Son, E. Janzén, and T. Ohshima, Phys. Status Solidi **245**, 1298 (2008).
[2] E. Janzén, A. Gali, A. Henry, I. G. Ivanov, B. Magnusson, and N. T. Son, in *Defects in Microelectronic Materials and Devices*, edited by D. M. Fleetwood, S. T. Pantelides, and R. D. Schrimpf (CRC Press, Boca Raton, Florida, 2009), p. 615.
[3] H. J. von Bardeleben, J. L. Cantin, L. Henry, and M. F. Barthe, Phys. Rev. B **62**, 10841 (2000).
[4] J. W. Steeds, G. A. Evans, L. R. Danks, S. Furkert, W. Voegeli, M. M. Ismail, and F. Carosella, Diamond Relat. Mater. **11**, 1923 (2002).
[5] M. Bockstedte, A. Mattausch, and O. Pankratov, Phys. Rev. B **68**, 205201 (2003).
[6] A. Gali, P. Deák, P. Ordejón, N. T. Son, E. Janzén, and W. J. Choyke, Phys. Rev. B **68**, 125201 (2003).
[7] L. Malerba and J. M. Perlado, Phys. Rev. B **65**, 045202 (2002).
[8] F. Gao and J. W. Weber, J. Appl. Phys. **94**, 4348 (2003).
[9] M. Bockstedte, A. Mattausch, and O. Pankratov, Phys. Rev. B **69**, 235202 (2004).
[10] G. Lucas and L. Pizzagalli, J. Phys.: Condens. Matter **19**, 086208 (2007).
[11] H. Nagasawa, K. Yagi, and T. Kawahara, J. Cryst. Growth **237-239**, 1244 (2002).
[12] H. Itoh, M. Yoshikawa, I. Nashiyama, S. Misawa, H. Okumura, and S. Yoshida, IEEE Trans. Nucl. Sci. **37**, 1732 (1990).
[13] H. Itoh, A. Kawasuso, T. Ohshima, M. Yoshikawa, I. Nashiyama, S. Tanigawa, S. Misawa, H. Okumura, and S. Yoshida, Phys. Status Solidi A **162**, 173 (1997).
[14] N. T. Son, P. N. Hai, and E. Janzén, Phys. Rev. B **63**, 201201(R) (2001).
[15] C. A. J. Ammerlaan, in *Landolt-Börnstein, New Series III/22b*, edited by O. Madelung and M. Schulz (Spinger-Verlag, Berlin, Heidelberg, 1989), p. 365.
[16] J. R. Morton and K. F. Preston, J. Magn. Reson. **30**, 577 (1978).
[17] G. H. Fuller, J. Phys. Chem. Ref. Data **5**, 835 (1976).
[18] H. J. Monkhorst and J. D. Pack, Phys. Rev. B **13**, 5188 (1976).
[19] D. M. Ceperley and B. J. Alder, Phys. Rev. Lett. **45**, 566 (1980).
[20] J. P. Perdew and A. Zunger, Phys. Rev. B **23**, 5048 (1981).
[21] G. Kresse and J. Hafner, Phys. Rev. B **49**, 14251 (1994); G. Kresse and J. Furthmüller, *ibid.* **54**, 11169 (1996).
[22] P. E. Blöchl, C. J. Först, and J. Schimpl, Bull. Mater. Sci. **26**, 33 (2003).
[23] P. E. Blöchl, Phys. Rev. B **50**, 17953 (1994).
[24] T. Umeda, Y. Ishitsuka, J. Isoya, N. T. Son, E. Janzén, N. Morishita, T. Ohshima, H. Itoh, and A. Gali, Phys. Rev. B **71**, 193202 (2005); T. Umeda, J. Isoya, T. Ohshima, N. Morishita, H. Itoh, and A. Gali, *ibid.* **75**, 245202 (2007).
[25] T. Umeda, N. T. Son, J. Isoya, E. Janzén, T. Ohshima, N. Morishita, H. Itoh, A. Gali, and M. Bockstedte, Phys. Rev. Lett. **96**, 145501 (2006).
[26] N. T. Son, P. Carlsson, J. ul Hassan, E. Janzén, T. Umeda, J. Isoya, A. Gali, M. Bockstedte, N. Morishita, T. Ohshima, and H. Itoh, Phys. Rev. Lett. **96**, 055501 (2006).
[27] A. Zywietz, J. Furthmüller, and F. Bechstedt, Phys. Rev. B **59**, 15166 (1999).
[28] B. Aradi, A. Gali, P. Deák, J. E. Lowther, N. T. Son, E. Janzén, and W. J. Choyke, Phys. Rev. B **63**, 245202 (2001).
[29] N. Mizuochi, S. Yamasaki, H. Takizawa, N. Morishita, T. Ohshima, H. Itoh, and J. Isoya, Phys. Rev. B **66**, 235202 (2002).
[30] E. Sörman, N. T. Son, W. M. Chen, O. Kordina, C. Hallin, and E. Janzén, Phys. Rev. B **61**, 2613 (2000).
[31] T. Hornos, N. T. Son, E. Janzén, and A. Gali, Phys. Rev. B **76**, 165209 (2007).